ISSN 1063-7834, Physics of the Solid State, 2007, Vol. 49, No. 8, pp. 1498–1506. © Pleiades Publishing, Ltd., 2007.
Original Russian Text © N.B. Ivanova, N.V. Kazak, C.R. Michel, A.D. Balaev, S.G. Ovchinnikov, A.D. Vasil'ev, N.V. Bulina, E.B. Panchenko, 2007, published in Fizika Tverdogo Tela, 2007, Vol. 49, No. 8, pp. 1427–1435.

MAGNETISM AND FERROELECTRICITY

Effect of Strontium and Barium Doping on the Magnetic State and Electrical Conductivity of $GdCoO_3$

N. B. Ivanova[a], N. V. Kazak[a], C. R. Michel[b], A. D. Balaev[a], S. G. Ovchinnikov[a], A. D. Vasil'ev[a], N. V. Bulina[a], and E. B. Panchenko[a]

[a] *Kirensky Institute of Physics, Siberian Division, Russian Academy of Sciences, Krasnoyarsk, 660036 Russia*
e-mail: nat@iph.krasn.ru

[b] *Departamento de Fisica, C.U.C.E.I., Universidade de Guadalajara, Guadalajara, Jalisco, 44430 Mexico*

Received November 30, 2006

Abstract—A coordinated investigation of the magnetic and electrical properties of polycrystalline cobalt oxide compounds $CdCoO_3$, $Gd_{0.9}Ba_{0.1}CoO_3$, and $Gd_{0.9}Sr_{0.1}CoO_3$ is carried out. Undoped $GdCoO_3$ reveals a low conductivity; a magnetic moment of 7.4 μ_B per molecule, which is less than the theoretical value for the Gd^{3+} ion; and an asymptotic Curie temperature of –6 K. Doping $GdCoO_3$ with barium and strontium to substitution of 10 at. % Gd brings about an increase in the conductivity and magnetic transitions at T = 300 K for $Gd_{0.9}Ba_{0.1}CoO_3$ and T = 170 K for $Gd_{0.9}Sr_{0.1}CoO_3$. The magnetization anomalies imply the formation of magnetic clusters. The behavior of the electrical conductivity at high temperatures suggests a variable activation energy. At low temperatures, Mott hopping conduction sets in.

PACS numbers: 72.80.Ga, 75.25.+z, 71.30.+h

DOI: 10.1134/S1063783407080161

1. INTRODUCTION

Cobalt oxide compounds based on $LaCoO_3$ have been attracting unwaning interest for over half the century as materials exhibiting a variety of unique physical properties, among them the appreciable magnetoresistance [1], anomalous behavior of the magnetic susceptibility [2, 3], thermopower [4–6], thermal expansion of the crystal lattice [7], and metal–insulator transitions [8–10]. A rich diversity of nontrivial physical effects manifests itself in compounds of this series in both iso- and nonisovalent substitutions of the rare-earth element [11–15].

The recent increasing interest in cobalt oxides stems from their promising application. The $LnCoO_3$-based compounds, where *Ln* stands for the lanthanum (*La*) or a lanthanide (Y, Sm, Gd, Ho, etc.), can be used to advantage in solid-state fuel cells (SOFC) [16], heterogeneous catalysts, oxygen membranes, and gas sensors [12]. The fairly large thermopower generated in cobaltites of rare-earth metals gives grounds to consider them as a viable alternative to traditional thermoelectric materials [17]. The availability of new spin and orbital degrees of freedom as compared to conventional semiconductors promises a broader spectrum of rare-earth metal cobaltite applications in semiconductor electronics and spintronics.

Considered from the standpoint of basic physics, $LaCoO_3$-based compounds are model materials to explore the part played by strong electronic correlations, hybridization, and charge and orbital ordering in formation of electronic states. Despite the more than half-a-century-long history of investigation of cobalt oxide compounds, some points in the nature and degree of stability of both the ground and higher-lying electronic states still remain subjects of debate.

The electronic state of a transition metal ion remains usually fixed, i.e., the total quantum number J, as well as the number of electrons in the 3*d* orbitals, has predetermined values. In the oxides under study here, the cobalt ion may not only reside in different valence states but have different spin states for a fixed valence. In many cases, the spin state of the cobalt ion varies with temperature. This transition is accompanied by a variation of the transport and magnetic properties. The nature of the ionic state and its effect on the physical properties are problems of fundamental importance in the investigation of the cobalt oxides, which is intimately connected with the existence of low-, high-, and intermediate-spin states.

The crystal field acting on a single CoO_6 octahedron splits the 3*d* orbitals into two e_g and three t_{2g} degenerate levels separated by 10 Dq. The 3*d* shell of the ion contains six (five) electrons for Co^{3+} (Co^{4+}). The Hund's rule suggests the $t_{2g}^4 e_g^2$ electronic configuration with a spin S = 2 to be preferable for Co^{3+}, and $t_{2g}^3 e_g^2$ with the spin S = 5/2, for Co^{4+}. The Hund energy J_H and crystal-field splitting 10 Dq compete. If neither energy dominates, one may conceive of the configuration $t_{2g}^5 e_g^1$ with

the spin $S = 1$ and $t_{2g}^4 e_g^1$ with $S = 3/2$ for the Co^{3+} and Co^{4+} ions, respectively. The electronic states of the Co^{3+} (Co^{4+}) ion with electronic configurations $t_{2g}^6 e_g^0$ ($t_{2g}^5 e_g^0$), $t_{2g}^4 e_g^2$ ($t_{2g}^3 e_g^2$), and $t_{2g}^5 e_g^1$ ($t_{2g}^4 e_g^1$) are called the low-spin (*LS*), the high-spin (*HS*), and the intermediate-spin (*IS*) states. It is the competition among the *LS*, *HS*, and *IS* states that gives rise to the unique transport and magnetic properties of $LaCoO_3$ and related compounds.

It is known that, at low temperatures ($T < 100$ K), $LaCoO_3$ is a nonmagnetic insulator with cobalt ions in the *LS* state. Many experimental studies dealing, for instance, with polarized neutron scattering [18] and Night shift [19], demonstrated that above 100 K the spin state of the Co^{3+} ion changes, but its character has not thus far been established. The Tanabe–Sugano diagrams make a crossover between the *LS* and *HS* terms in a d^6 ion with a crystal field change of 10 *Dq* possible [20]. By contrast, experiments suggest rather the intermediate spin state [2].

In addition to a decrease in the temperature, the *LS* state can be stabilized also through application of an external [21–23] or chemical pressure [24] by replacing the lanthanum with another element with a smaller ionic radius. This should be attributed to the record-high compressibility of the Co–O bond in cobalt oxide compounds [21]. It was suggested [25] that in all compounds of the $LnCoO_3$ series, with the exclusion of the case with Ln = La, the Co^{3+} ion remains in the nonmagnetic low-spin state up to room temperature. This suggestion was substantiated experimentally [15, 24].

Despite a large number of publications dealing with cobaltites of rare-earth metals, only the basic compound $LaCoO_3$ may be considered presently as studied well enough; note, however, that even this material, more than half a century after the beginning of its investigation, continues to plague the researcher with novel unexpected effects. Indeed, quite recently it was found that even a very low doping of $LaCoO_3$ with strontium, for substitution concentrations $x < 0.005$, brings about a strong change in its spin state [26]. Experimental data on other members of the $LnCoO_3$ series are fairly scarce, particularly in the low-temperature domain. At the same time, adequate knowledge of the properties of these compounds is needed to increase their application potential. The present publication reports on an experimental low-temperature study of the $GdCoO_3$ compound with partial substitution of the rare-earth ion with the Ba and Sr divalent ions.

2. SAMPLES AND EXPERIMENTAL TECHNIQUES

The polycrystalline samples were prepared by the sol–gel technology [9], in which the cobalt and gadolinium nitrates taken in stoichiometric ratio were dissolved in deionized water and dried subsequently at 90°C for 6 h. The powder samples thus obtained were annealed at 300°C in air, pressed, and annealed again. In this way, $GdCoO_3$, $Gd_{0.9}Ba_{0.1}CoO_3$ and $Gd_{0.9}Sr_{0.1}CoO_3$ samples were prepared. The pressed samples were rectangular parallelepipeds measuring $4 \times 2 \times 1$ mm.

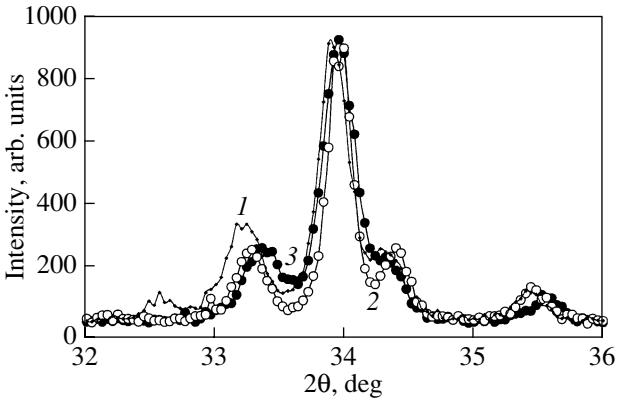

Fig. 1. Fragments of the x-ray diffraction patterns of (*1*) $GdCoO_3$, (*2*) $Gd_{0.9}Ba_{0.1}CoO_3$, and (*3*) $Gd_{0.9}Sr_{0.1}CoO_3$ samples.

The x-ray diffraction patterns of the samples were obtained on a DRON-4 diffractometer.

We measured thermopower at room temperature, temperature dependences of the electrical resistivity from 80 to 400 K, temperature dependences of static magnetization within the temperature range of 4.2–300 K, and magnetization curves at different temperatures in magnetic fields of up to 12 kOe.

The electrical resistance of the samples was measured between clamp-on contacts applied with indium amalgam. The ohmic nature of the contacts was checked by monitoring the *I–V* characteristic. The sample with contacts was placed in a glass gas-flow cryostat fixed between the poles of a laboratory magnet and blown around by a properly controlled jet of the cooling gas. The electrical resistance was measured by the standard four-probe technique.

The sample magnetization was determined with a computerized vibrating-coil magnetometer with a superconducting solenoid.

3. EXPERIMENTAL RESULTS

3.1. Crystal Structure

X-ray diffraction showed all the samples to have an orthorhombic distorted perovskite-like structure typical of compounds of the $LnCoO_3$ series. The lattice parameters found agree with literature data [27]. Doping brings about redistribution of peak intensities in the diffraction patterns, which indicates additional lattice distortions caused by introduction of the impurities. For comparison, Fig. 1 shows fragments of the diffraction patterns corresponding to the scattering angles $2\theta = 32°–36°$.

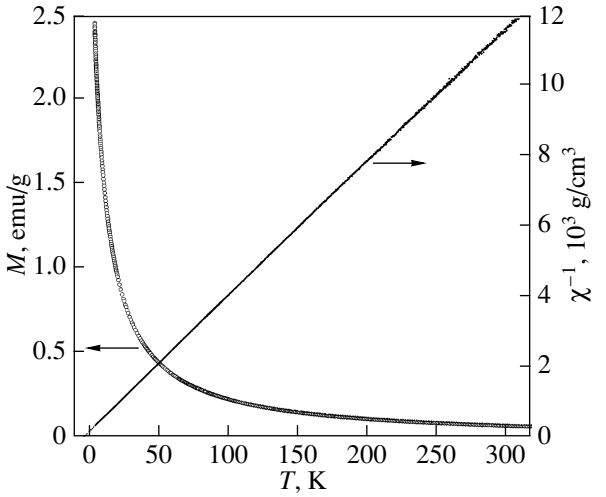

Fig. 2. Temperature dependences of the magnetization and the reciprocal of the magnetic susceptibility of $GdCoO_3$ in the magnetic field $H = 1$ kOe.

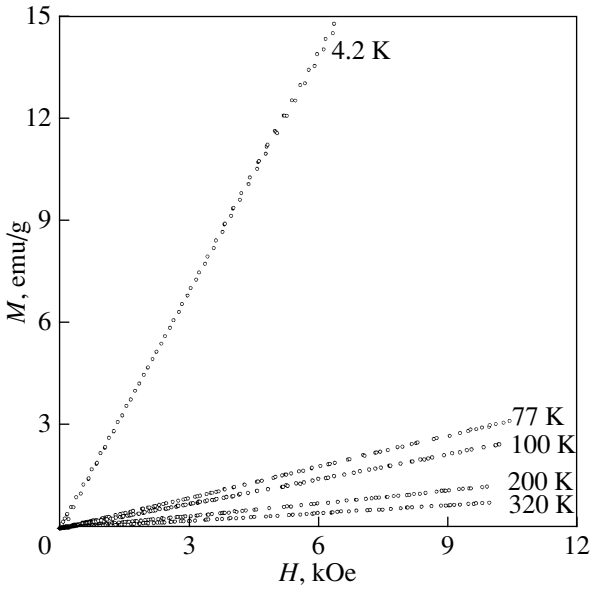

Fig. 3. Magnetization lines of $GdCoO_3$ at different temperatures.

3.2. Magnetization

Figure 2 displays the temperature dependence of the magnetization $M(T)$ of an undoped $GdCoO_3$ sample in a magnetic field $H = 1$ kOe. The magnetization increases strongly at low temperatures. On the whole, the $M(T)$ graph is monotonic and has no features. The dependence of the reciprocal of the magnetic susceptibility is well fitted by a straight line, thus permitting one to derive the asymptotic Curie temperature $\theta_0 \approx -6$ K and the effective magnetic moment per formula unit, $\mu_{eff} \approx 7.38\mu_B$, where μ_B is the Bohr magneton.

Figure 3 plots magnetization lines of a $GdCoO_3$ sample at different temperatures. In fields of up to 12 kOe, all these dependences are fitted by straight lines.

In contrast to the undoped $GdCoO_3$ compound, the temperature dependences of magnetization of the doped $Gd_{0.9}Ba_{0.1}CoO_3$ and $Gd_{0.9}Sr_{0.1}CoO_3$ samples exhibit clearly pronounced features in the form of maxima near $T_{max1} = 250$ K for the first, and $T_{max2} = 100$ K for the second sample. Figure 4 plots these relations for a magnetic field $H = 1$ kOe. The temperature at which the magnetic transition sets in is approximately 300 K for $Gd_{0.9}Ba_{0.1}CoO_3$ and 170 K for $Gd_{0.9}Sr_{0.1}CoO_3$. As is seen from a comparison of the $M(T)$ curves for $Gd_{0.9}Ba_{0.1}CoO_3$ obtained in different fields (Fig. 5), the maximum in $M(T)$ is most clearly pronounced in weak magnetic fields. The FC (field-cooled) and ZFC (zero-field-cooled) curves also behave in different ways. Figure 5a displays the temperature dependence of the reciprocal of the magnetization of the sample, which scales as $1/\chi$. This dependence is nonmonotonic, passes through a minimum at $T = 246$ K, and is practically linear at the temperatures 280–300 K corresponding to the onset of the magnetic transition. Approximation of the linear part of the graph yields $\theta_1 = 276$ K for the asymptotic Curie temperature and $2.07\mu_B$ for the effective magnetic moment per molecule.

At low temperatures, the behavior of $M(T)$ of the barium-doped gadolinium cobaltite approaches that of the undoped $GdCoO_3$ sample, but the magnetization of the doped sample measured at 4.2 K in different fields is higher by 11–13%, a hardly expected observation, because 10% of the Gd^{3+} ions possessing a large magnetic moment are replaced in this sample with nonmagnetic Ba^{2+}. The temperature dependence of the reciprocal of the magnetic susceptibility of $Gd_{0.9}Ba_{0.1}CoO_3$ follows at low temperatures the Curie–

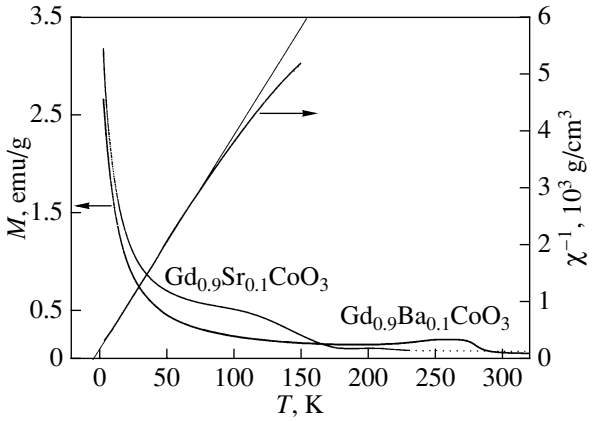

Fig. 4. Temperature dependences of the magnetization of $Gd_{0.9}Ba_{0.1}CoO_3$ and $Gd_{0.9}Sr_{0.1}CoO_3$ in the magnetic field $H = 1$ kOe and the reciprocal of the magnetic susceptibility of $Gd_{0.9}Ba_{0.1}CoO_3$.

Weiss law, just as that of $GdCoO_3$ does (Fig. 4). The low-temperature linear part of the straight line approximating the $1/\chi$ course yields for the asymptotic Curie temperature $\theta_0 = -5.5$ K and $\mu_{eff} \approx 7.48\mu_B$, values close to those for the undoped sample, but the magnetic moment of the molecule in this case is slightly larger. As the temperature increases, one observes deviations from the Curie–Weiss law, starting from $T \approx 85$ K. The decrease in the slope of the tangent to the curve correlates with the increase in the magnetic moment with temperature.

Far enough from the critical temperatures corresponding to the maximum in $M(T)$, the dependences of the magnetization of $Gd_{0.9}Ba_{0.1}CoO_3$ on magnetic field H are very nearly linear, just as for $GdCoO_3$. In the vicinity of the temperature T_{max1}, however, the magnetization curve exhibits a hysteresis loop. These loops are shown in Figs. 6a–6d for four different temperatures. The magnetization does not undergo a distinct jump in the vicinity of the coercive field.

Similar hysteresis loops in magnetization are observed for the $Gd_{0.9}Sr_{0.1}CoO_3$ sample at temperatures near 100 K (Fig. 7). The only difference from the barium-doped sample consists in that, in the low-temperature domain, the loop does not disappear down to $T = 4.3$ K. Besides, the magnetization of the strontium-doped sample at this temperature is the largest as compared to the other two samples and exceeds by about 30% that of the undoped sample.

3.3. Electrical Conductivity

Thermopower measurements show all the samples under study to have *p* conduction.

Measurements of the electrical resistivity revealed that the undoped $GdCoO_3$ sample has a fairly high room-temperature resistivity ($\rho \sim 10^5$ Ω m), which grows still more with decreasing temperature. Thus, at low temperatures undoped $GdCoO_3$ may be classed among dielectrics. Our value of the electrical resistivity at room temperature is higher than the one reported earlier for $GdCoO_3$ in [8], which apparently should be assigned to different technologies of sample preparation followed and, hence, different oxygen vacancy concentrations, which affect strongly the resistivity. The state of grain boundaries is also of considerable importance, because we deal here with polycrystalline granular materials. The electrical resistivity of the $Gd_{0.9}Sr_{0.1}CoO_3$ sample at room temperature is, in order of magnitude, $\rho \sim 10^{-2}$ Ω m, and that of the $Gd_{0.9}Ba_{0.1}CoO_3$ sample, $\sim 10^{-1}$ Ω m.

The resistivity of doped samples grows markedly with decreasing temperature. Figure 8 plots the natural logarithm of the electrical conductivity $\sigma = 1/\rho$ as a function of the reciprocal of the temperature $10^3/T$ for the $Gd_{0.9}Ba_{0.1}CoO_3$ and $Gd_{0.9}Sr_{0.1}CoO_3$ samples. We readily see that the graphs deviate substantially from the simple

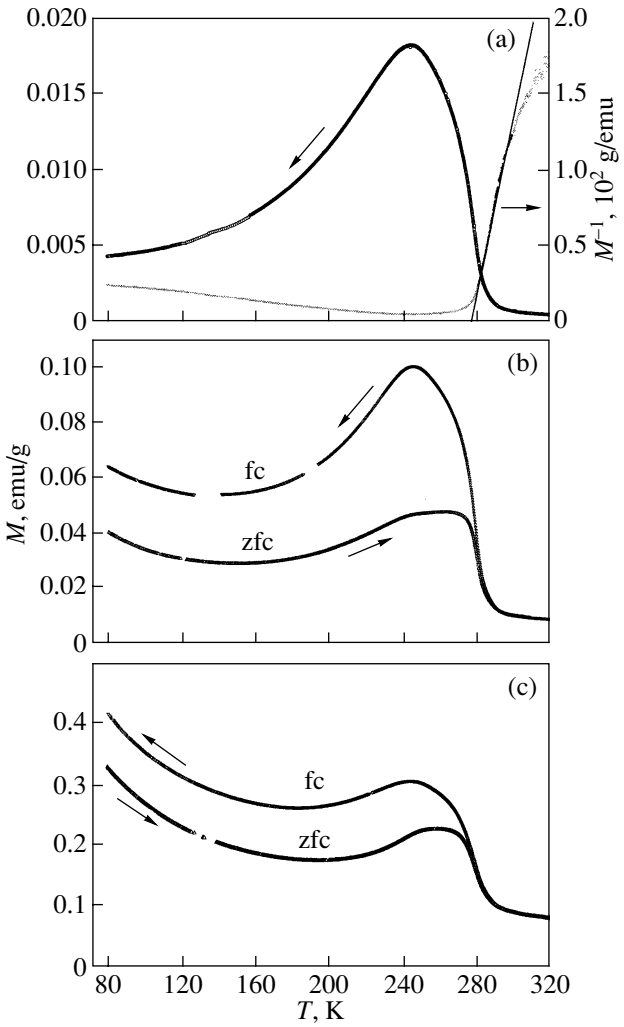

Fig. 5. Anomaly in the temperature dependence of the magnetization of $Gd_{0.9}Ba_{0.1}CoO_3$ in magnetic fields H = (a) 0, (b) 0.1, and (c) 1.0 kOe. Panel (a) shows the temperature dependence of the reciprocal of the magnetization.

law of activated conductivity $\sigma = \sigma_{01}\exp(-\Delta/kT)$ (Δ is the activation energy, and k in the Boltzmann constant) which would require the lines in Fig. 8 to be linear. The varying activation energy is attributed [28] to anomalous temperature-induced expansion of the lattice in $LnCoO_3$ compounds. The temperature dependences of the activation energy calculated [28] as a derivative of the $\sigma(T)$ relation and of the linear expansion coefficient α correlate well. Both these curves pass through a maximum in the 400–800-K region, depending on the lanthanide ion. Because our measurements were conducted at lower temperatures, no maximum was observed in the $\Delta(T)$ graph; as for the low-temperature behavior of this quantity, it correlates with the data of [28]. The temperature dependence of the activation energy Δ derived from the slope of the tangent to the curves in Fig. 8 is shown graphically in Fig. 9. The room-temperature values of Δ found to be 0.17 and

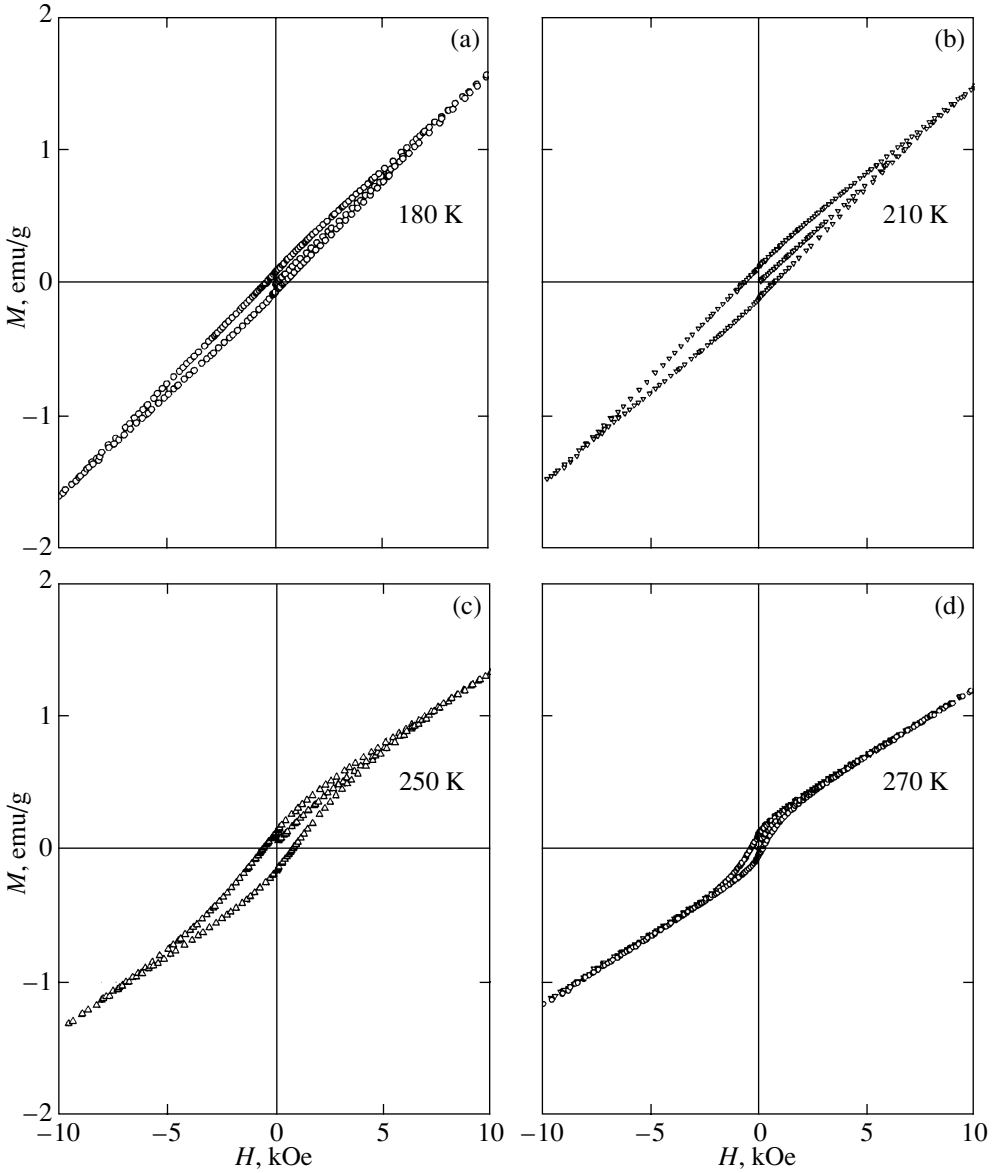

Fig. 6. Hysteresis loop in the magnetization of $Gd_{0.9}Ba_{0.1}CoO_3$ at different temperatures.

0.24 eV for the $Gd_{0.9}Sr_{0.1}CoO_3$ and $Gd_{0.9}Ba_{0.1}CoO_3$ samples, respectively, are close to the value $\Delta \sim 0.2$ eV obtained in [28] for $GdCoO_3$ at the same temperature.

The thermal expansion of the lattice was studied in [28] for temperatures above 100–150 K. It was shown that, at low temperatures, the linear expansion coefficient is small and that it depends on the temperature weaker than is the case with the high-temperature region. The high values of the electrical resistivity, combined with the presence in the lattice of randomly distributed substituting alkaline-earth ions, suggest Anderson localization of carriers in the samples under study and the onset of Mott variable-range hopping (VRH) conduction described by the expression [29]

$$\sigma = \sigma_{0.2}\exp(-T_0/T)^{1/4}.$$

The quantity T_0 defines the characteristic hopping-conduction temperature, and the value of the constant σ_{02} depends on the magnitude of electron-phonon coupling. Figure 10 plots $\ln\sigma$ vs. temperature raised to –1/4 power. We readily see that the Mott law describes quite satisfactorily the experimental data obtained at temperatures $T < 300$ K. At higher temperatures, as supposed in [28], a transition from the Mott law of conduction to the activated regime with a variable activation energy apparently takes place.

4. RESULTS AND DISCUSSION

Our experimental studies of the cobaltite $GdCoO_3$ and of doped $GdCoO_3$-based compounds have revealed specific features in the behavior of the magnetic prop-

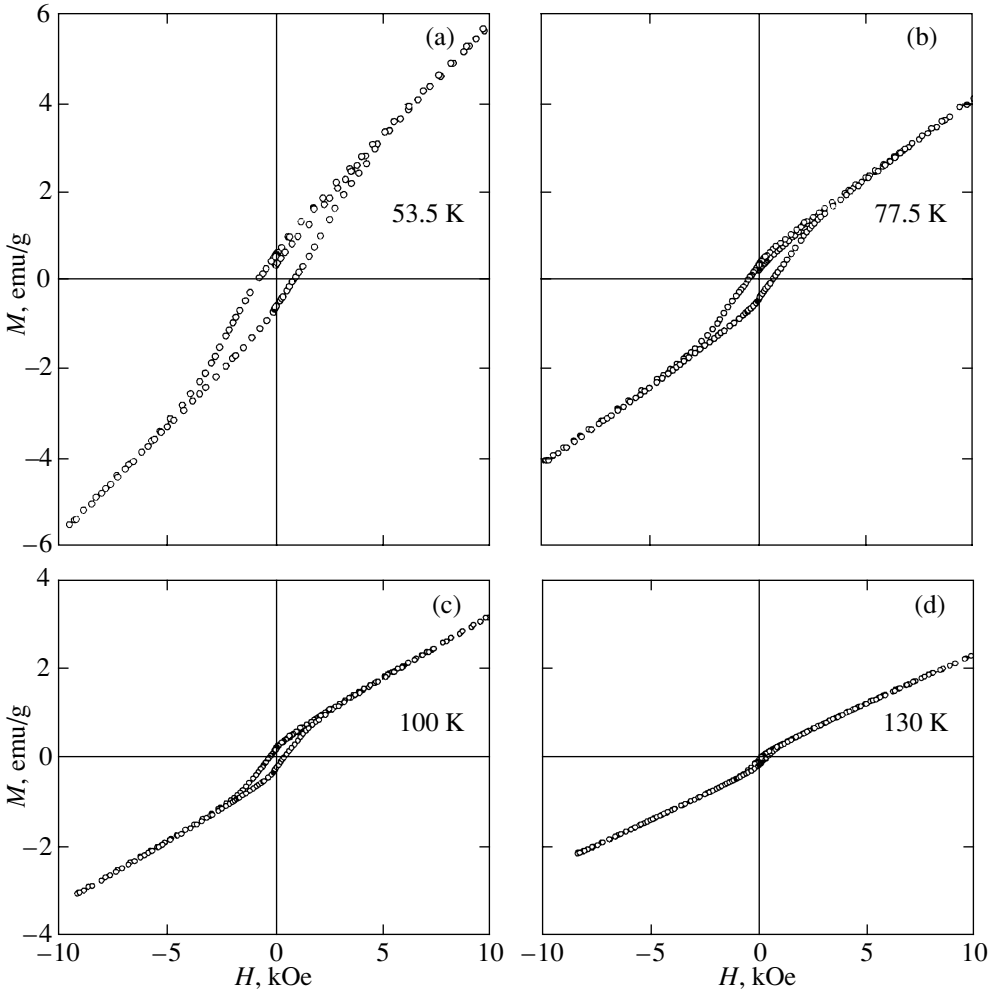

Fig. 7. Hysteresis loop in the magnetization of $Gd_{0.9}Sr_{0.1}CoO_3$ at different temperatures.

erties of these materials. As for the undoped compound $GdCoO_3$, we have in mind its low-temperature magnetization, because the stoichiometric compound contains magnetic ions of two kinds, the trivalent gadolinium and cobalt. If we assume, as discussed earlier, that in the temperature region involved, all trivalent cobalt ions reside in the nonmagnetic *LS* state, then the total observed magnetic moment should be attributed to the practically noninteracting Gd^{3+} ions. In the absence of interaction, the system under study should behave purely paramagnetically, with $\theta = 0$ K and the theoretical value $\mu_{eff} = 7.94\ \mu_B$. Experiment reveals, however, negative values of θ and a substantially smaller value of μ_{eff}. A similar behavior of magnetic systems containing Gd^{3+} ions, i.e., a combination of a reduced magnetic moment with negative values of the paramagnetic Curie temperature, was observed more than once in Gd_2O_3-based oxide glasses [30–33]. As follows from our studies and data reported in [30–33], Gd^{3+} ions in the systems studied, rather than being fully isolated from one another, interact, with this interaction containing an antiferromagnetic component. The exchange interaction J quoted in the literature is, as a rule, not large. Indeed, calculations [31] performed in the model of a conventional Heisenberg antiferromagnet yielded $J/k = -0.135$ K, while our result is $J/k = -0.1$ K.

Deviation from stoichiometry is known to play a major part in formation of the properties of metal oxides. This mechanism is particularly significant in polycrystalline materials. Compounds in the $LnCoO_3$ series are, as a rule, oxygen deficient [14, 34]. It was shown, for instance, that annealing of $Sr_{0.775}Y_{0.225}CoO_3$ samples in an oxygen environment brings about a radical change in their magnetic properties [15]. Charge neutrality considerations suggest that breakdown of stoichiometry by the formation of oxygen vacancies should give rise to creation of divalent Co^{2+} ions in the $GdCoO_3$ lattice. These ions can apparently act as nuclei of antiferromagnetic microregions in the compound under study.

The reduction of the Gd^{3+} magnetic moment as compared to its theoretical value may be caused also by

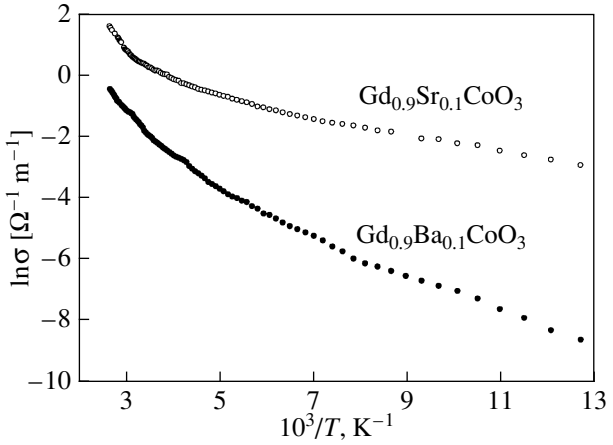

Fig. 8. Natural logarithm of the electrical conductivity as a function of the reciprocal of the temperature.

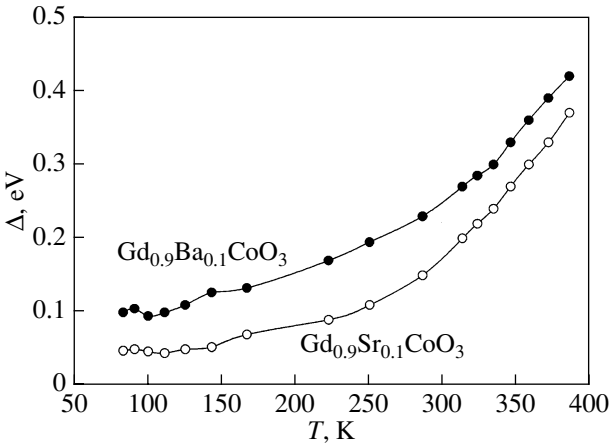

Fig. 9. Temperature dependences of the activation energy.

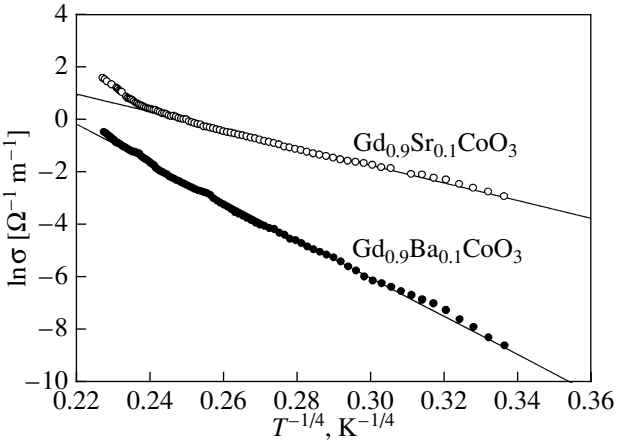

Fig. 10. Natural logarithm of the electrical conductivity as a function of the temperature raised to –1/4 power.

crystal field splitting of its ground state, the octet $^8S_{7/2}$. Experimental observation of this splitting by paramagnetic resonance and its possible mechanisms are discussed in [35]. While both the experimentally observed and the theoretical value of the splitting does not exceed 1 K, it can affect the low-temperature magnetization through activation of the spin–orbit interaction.

The totality of experimental data on the magnetization of the $Gd_{0.9}Ba_{0.1}CoO_3$ sample indicates that, at low temperatures, $T < 100$ K, it approaches in behavior the undoped sample, but the absolute values of the magnetization reached were found unexpectedly to be 1–13% larger. To preserve charge neutrality, the nonisovalent substitution of divalent barium for the trivalent gadolinium should bring about creation of an equivalent number of Co^{4+} ions, as well as of holes which initiate ferromagnetic ordering in the regions where they appear. In these conditions, the ground state of Co^{4+} and of the neighboring Co^{3+} ions may be not the low-spin one, because nonisovalent ions appear primarily in the vicinity of local lattice distortions, while the crystal field depends critically on interatomic separation.

Thus, doping with barium cannot be reduced simply to the effect of diamagnetic dilution. The formation of quadrivalent cobalt ions should give rise to new kinds of exchange interactions. It is the onset of magnetic order in $Gd_{0.9}Ba_{0.1}CoO_3$ and $Gd_{0.9}Sr_{0.1}CoO_3$ samples at $T = 290$ K for the former and $T = 170$ K for the latter compound that substantiate the existence of these interactions. This phenomenon is characteristic of compounds in the $LnCoO_3$ series, in which doping with strontium and barium can bring about spin-glass and even ferromagnetic ordering [13–15, 36]. The record-high magnetic ordering temperature observed is 335 K for $Y_{1-x}Sr_xCoO_3$ [36].

A similar magnetic phase transition initiated by substitution of gadolinium with barium was observed earlier for the $Gd_{0.5}Ba_{0.5}CoO_3$ compound [13]. The transition to the magnetically ordered phase in $Gd_{0.5}Ba_{0.5}CoO_3$ occurs at a temperature very close to the one observed for $Gd_{0.9}Ba_{0.1}CoO_3$, which suggests the same strength and, probably, the same nature of the exchange interaction in these two materials. The exchange interaction is $J/k \sim 90$ K. The maximum magnetization in $Gd_{0.5}Ba_{0.5}CoO_3$ at $T_{max1} \sim 250$ K is, however, 18 (!) times larger than the value obtained by us for $Gd_{0.9}Ba_{0.1}CoO_3$. This may probably imply formation of extended ferromagnetically ordered clusters around divalent alkaline-earth elements.

5. CONCLUSIONS

While information on the static magnetization is clearly insufficient for precise establishment of the nature of magnetic ordering in $Gd_{0.9}Ba_{0.1}CoO_3$ and $Gd_{0.9}Sr_{0.1}CoO_3$ in the vicinity of the critical temperatures, the temperature and magnetic field dependences

of the magnetization suggest that we are dealing here most probably with the cluster spin-glass state rather than with volume ferromagnetism.

One could point out more than one mechanism that could be responsible for the formation of the magnetic state in $Ln\mathrm{CoO}_3$ involving alkaline-earth substitution. First, introduction of an alkaline-earth ion with a large ionic radius brings about a local lattice distortion and, hence, a change in relative magnitude of crystal field 10 Dq and the Hund exchange energy J_H, which may initiate a change in the spin state of the cobalt ions. Second, an increase in the hole concentration and appearance of Co^{4+} ions under nonisovalent substitution of a rare- with an alkaline-earth one should create new kinds of exchange interactions. Finally, this violation of sample stoichiometry caused primarily by the presence of oxygen vacancies gives rise now to formation of the divalent cobalt Co^{2+}. The possibility of the onset of charge and orbital ordering in doped rare-earth metal cobaltites was also considered [10]. Thus, the $GdCoO_3$-based compounds considered here can support simultaneous existence of cobalt ions in different valence and spin states. The sign and strength of exchange interactions depend strongly on interatomic distances, therefore, systems with local disorder created by oxygen vacancies and dopants will be governed by exchange interactions of opposite signs. We see that, at low temperatures, $GdCoO_3$ and $Gd_{0.9}Ba_{0.1}CoO_3$ samples are dominated by antiferromagnetic interaction manifesting itself against the background of the conventional gadolinium 4f paramagnetism, while about the critical temperatures of 170 and 290 K magnetic order with a ferromagnetic component sets in $Gd_{0.9}Sr_{0.1}CoO_3$ and $Gd_{0.9}Ba_{0.1}CoO_3$ compounds.

As for the electrical conductivity, the doping-induced hole creation should certainly give rise to its growth, exactly what is observed experimentally both in the present and in the preceding studies [14, 16]. No clearly pronounced transition of the metal–insulator type is, however, observed in the systems studied, because at the dopant concentration chosen ($x = 0.1$) the conduction band holes reside apparently predominantly in magnetically ordered clusters around the impurity and the percolation threshold has not yet been reached. At low temperatures, the local disorder caused by the impurity favors the onset of Mott variable-range hopping conduction. Above room temperature it is apparently the activated mechanism of conduction that dominates. The activation energy grows with increasing temperature due to the anomalous linear thermal expansion of the crystal lattice.

ACKNOWLEDGMENTS

This study was supported of the DPS program "Strong Electronic Correlations" and the Russian Foundation for Basic Research.

REFERENCES

1. G. Briceno, H. Chang, X. Sun, P. G. Shultz, and X.-D. Xiang, Science (Washington) **270**, 273 (1995).
2. C. Zobel, M. Kriener, D. Bruns, J. Baier, M. Gruninger, and T. Lorenz, Phys. Rev. B: Condens. Matter **66**, 020402 (2002).
3. R. Caciuffo, D. Rinaldi, G. Barucca, J. Mira, J. Rivas, M. A. Senaris-Rodrigues, P. G. Radaelli, D. Fiorani, and J. B. Goodenough, Phys. Rev. B: Condens. Matter **59**, 1068 (1999).
4. A. Maignan, V. Caignaert, B. Raveau, D. Khomskii, and G. Sawatsky, Phys. Rev. Lett. **93**, 026401 (2004).
5. K. Berggold, M. Kriener, C. Zobel, A. Reichl, M. Reuther, R. Muller, A. Freimuth, and T. Lorenz, Phys. Rev. B: Condens. Matter **72**, 155116 (2005).
6. J.-W. Moon, W.-S. Seo, H. Okabe, T. Okawa, and K. Koumoto, J. Mater. Chem. **10**, 2007 (2000).
7. M. Kriener, M. Braden, D. Sneff, O. Zabara, and T. Lorenz, cond-mat/0605721 (2006).
8. G. Thornton, F. C. Morrison, S. Partington, B. C. Tofield, and D. E. Williams, J. Phys. C: Solid State Phys. **21**, 2871 (1988).
9. Y. Tokura, Y. Okimoto, S. Yamaguchi, H. Taniguchi, T. Kimura, and H. Takagi, Phys. Rev. B: Condens. Matter **58**, 1699 (1998).
10. Y. Morimoto, M. Takeo, X. J. Liu, T. Akimoto, and A. Nakamura, Phys. Rev. B: Condens. Matter **58**, R13334 (1998).
11. J. Baier, S. Jodlauk, M. Kriener, A. Reichl, C. Zobel, H. Rierspel, A. Freimuth, and T. Lorenz, Phys. Rev. B: Condens. Matter **71**, 014443 (2005).
12. C. R. Michel, A. S. Sago, H. Guzman-Colin, E. R. Lopes-Mena, D. Lardizabal, and O. S. Buassi-Monroy, Mater. Res. Bull. **39**, 2295 (2004).
13. I. O. Troyanchuk, N. V. Kasper, D. D. Khalyavin, H. Szymczak, R. Szymczak, and M. Baran, Phys. Rev. B: Condens. Matter **58**, 2418 (1998).
14. M. Kriener, C. Zobel, A. Reichl, J. Baier, M. Cwik, K. Berggold, H. Kierspel, O. Zabara, A. Freimuth, and T. Lorenz, Phys. Rev. B: Condens. Matter **69**, 094417 (2004).
15. K. Yoshii and A. Nakamura, Physica B (Amsterdam) **281–282**, 514 (2000).
16. Y. Takeda, H. Ueno, N. Imanishi, O. Yamamoto, N. Sammes, M. B. Phillips, Solid State Ionics **86–88**, 1187 (1996).
17. S. Maekawa, T. Tohyama, S. E. Barnes, S. Ishihara, W. Koshibae, and G. Khaliullin, *Physics of Transition Metal Oxides* (Springer, New York, 2004).
18. K. Asai, P. Gehring, H. Chou, and G. Shirane, Phys. Rev. B: Condens. Matter **40**, 10982 (1989).
19. M. Itoh, M. Sugahara, I. Natori, and K. Matoya, J. Phys. Soc. Jpn. **64**, 3967 (1995).
20. Y. Tanabe and S. Sugano, J. Phys. Soc. Jpn. **9**, 766 (1954).
21. T. Vogt, J. A. Hriljac, N. C. Hyatt, and P. Woodward, Phys. Rev. B: Condens. Matter **67**, 140401 (2003).
22. R. Lengsdorf, M. Ait-Tahar, S. S. Saxena, M. Ellerby, D. I. Khomskii, H. Micklitz, T. Lorenz, and M. M. Abd-

Elmeguid, Phys. Rev. B: Condens. Matter **69**, 140403 (2004).

23. G. Vanko, J. P. Rueff, A. Mattila, Z. Nemeth, and A. Shukla, Phys. Rev. B: Condens. Matter **73**, 024424 (2006).
24. I. A. Nekrasov, S. V. Streltsov, M. A. Korotin, and V. I. Anisimov, Phys. Rev. B: Condens. Matter **68**, 235113 (2003).
25. X. Liu and C. T. Prewitt, J. Phys. Chem. Solids **52**, 441 (1991).
26. A. Podlesnyak, K. Conder, E. Pomjakushina, A. Mirmelstein, P. Allenspach, and D. I. Khomskii, cond-mat/0609247 (2006).
27. G. Demazeau, M. Pouchard, and P. Hagenmuller, J. Solid State Chem. **9**, 202 (1974).
28. K. Knížek, Z. Jirák, J. Hejtmánek, M. Veverka, and M. Maryško, cond-mat/0503104 (2005).
29. N. F. Mott, *Metal-Insulator Transition* (Taylor and Francis, London, 1974; Nauka, Moscow, 1979).
30. C. J. Schinkel and W. D. van Amstel, Phys. Lett. A **44**, 467 (1973).
31. R. M. Moon and W. C. Koehler, Phys. Rev. B: Solid State **11**, 1609 (1975).
32. I. Ardelean, E. Burzo, D. Mitulesku-Ungur, and S. Simon, J. Non-Cryst. Solids **146**, 256 (1992).
33. E. Culea, A. Pop, and I. Cosma, J. Magn. Magn. Mater. **157/158**, 163 (1996).
34. W. Kobayashi, S. Ishiwata, I. Terasaki, M. Takano, I. Grigoraviciute, H. Yamauchi, and M. Karppinen, Phys. Rev. B: Condens. Matter **72**, 104408 (2005).
35. M. M. Abraham, L. A. Boatner, C. B. Finch, E. J. Lee, and R. A. Weeks, J. Phys. Chem. Solids **28**, 81 (1967).
36. K. Yoshii, M. Mizumaki, Y. Saitoh, and A. Nakamura, J. Solid State Chem. **152**, 577 (2000).

Translated by G. Skrebtsov